UNCLASSIFIED

AD NUMBER

AD482038

LIMITATION CHANGES

TO:

Approved for public release; distribution is unlimited.

FROM:

**Distribution authorized to U.S. Gov't. agencies and their contractors;
Administrative/Operational Use; MAY 1966. Other requests shall be referred to Arnold Engineering Development Center, Arnold AFB, TN 37389.**

AUTHORITY

USAF ltr, 4 Apr 1973

THIS PAGE IS UNCLASSIFIED

ARCHIVE COPY
DO NOT LOAN

THE IMPACT OF THIN DISKS INTO SEMI-INFINITE ALUMINUM TARGETS

J. J. Payne

ARO, Inc.

May 1966

This document has been approved for public release its distribution is unlimited. Per A. F. Letter dated 4 April '73 signed William A. Cole.

~~This document is subject to special export controls and each transmittal to foreign governments or foreign nationals may be made only with prior approval of NASA.~~

PROPERTY OF U. S. AIR FORCE
AEDC LIBRARY
AF 40(600)1200

AEDC TECHNICAL LIBRARY
5 0720 00031 2407

VON KÁRMÁN GAS DYNAMICS FACILITY
ARNOLD ENGINEERING DEVELOPMENT CENTER
AIR FORCE SYSTEMS COMMAND
ARNOLD AIR FORCE STATION, TENNESSEE

NOTICES

When U. S. Government drawings specifications, or other data are used for any purpose other than a definitely related Government procurement operation, the Government thereby incurs no responsibility nor any obligation whatsoever, and the fact that the Government may have formulated, furnished, or in any way supplied the said drawings, specifications, or other data, is not to be regarded by implication or otherwise, or in any manner licensing the holder or any other person or corporation, or conveying any rights or permission to manufacture, use, or sell any patented invention that may in any way be related thereto.

Qualified users may obtain copies of this report from the Defense Documentation Center.

References to named commercial products in this report are not to be considered in any sense as an endorsement of the product by the United States Air Force or the Government.

THE IMPACT OF THIN DISKS INTO SEMI-INFINITE ALUMINUM TARGETS

J. J. Payne
ARO, Inc.

This document is subject to special export controls and each transmittal to foreign governments or foreign nationals may be made only with prior approval of NASA.

AF - AEDC
Arnold AFB Tenn

This document has been approved for public release and its distribution is unlimited.
Per D F Little
4 April 1973
Capt William D. Cole

FOREWORD

The work reported herein was done at the request of the National Aeronautics and Space Administration (NASA), Marshall Space Flight Center (MSFC), under Project SUPER (Support Program for Extra-terrestrial Research), and performed under System 920E, Project 9514.

The results of tests presented were obtained by ARO, Inc. (a subsidiary of Sverdrup and Parcel, Inc.), contract operator of the Arnold Engineering Development Center (AEDC), Air Force Systems Command (AFSC), Arnold Air Force Station, Tennessee, under Contract AF 40(600)-1200. The tests were conducted from April 10 through August 14, 1965, under ARO Project No. VS1443, and the manuscript was submitted for publication on January 26, 1966.

The author wishes to acknowledge the assistance of Mrs. Linda Welch for her work in the velocity and crater dimension determinations.

This technical report has been reviewed and is approved.

John W. Hitchcock
Major, USAF
AF Representative, VKF
DCS/Test

Jean A. Jack
Colonel, USAF
DCS/Test

ABSTRACT

Hypervelocity impact tests have been performed using aluminum targets and projectiles comprising low-fineness-ratio disks (ℓ/d from 0.1 to 1.0) of 1100-0 aluminum, commerically pure titanium, mild steel, and Kennertium® (97.6 percent tungsten). To ensure the desired projectile attitudes upon impact, rifled launch tubes were used to produce spin stabilization. These tubes allowed the establishment of the desired projectile orientation (their planar surface normal to the flight path) and the removal of a multipieced sabot without a mechanical stripping device. Cratering data for impact velocities from 11,300 to 26,200 fps indicate that the steady-state stage of hypervelocity impact of disks is important and that steady-state duration times of at least 6 μsec are significant.

CONTENTS

ILLUSTRATIONS

TABLES

NOMENCLATURE

D_c	Diameter of crater
d	Diameter of projectile
ℓ	Length of projectile
P_D	Depth of penetration of disk
P_S	Depth of penetration of sphere
S_t	Target deformation stress
t	Time
V_c	Crater volume
V_p	Projectile velocity
ρ_p	Projectile density
ρ_t	Target density

SECTION I
INTRODUCTION

The program reported herein was conducted in the hypervelocity impact range (Armament Test Cell, Hyperballistic (S1)) of the von Karmán Gas Dynamics Facility (VKF). The program required impacts of low-fineness-ratio disks into aluminum targets at velocities of from 13,000 to 26,000 fps. The program further required that the planar surface of the projectile be perpendicular to the flight line. The experimental data obtained were projectile velocity and crater volume, diameter, and depth.

The purpose of this program was to launch disks of varying ℓ/d ratios and of different materials at different velocities to produce the same initial pressures in aluminum targets. It was thought that by selecting the length of the projectile, hence the time before the pressure pulse is relieved, identical pressure pulses could be created by the various projectiles. This program was but a part of cratering studies sponsored by MSFC, where the overall aim is to develop a theoretical model, with experimental verifications, for impact and cratering processes.

The purpose of this report is to discuss the actual cratering process rather than to attempt to correlate any of the cratering parameters to initial impact pressures.

SECTION II
APPARATUS

2.1 LAUNCHER AND RANGE

Armament Test Cell S1 consists of: (1) a two-stage launcher, (2) an expansion tank to absorb muzzle blast and to provide space for separation of the projectile from the sabot, (3) a connecting tube which has provision for measuring projectile velocity, and (4) a target chamber. During the course of the test, two launcher configurations were used. The first employed a 10-ft-long powder chamber and a 10-ft-long pump tube of 2-in. ID. The second configuration is shown with the range in Fig. 1. This launcher employed a 5-ft-long powder chamber and a 20-ft long pump tube of 2-1/2-in. ID and was used primarily to obtain the higher velocities.

To ensure desired projectile attitude on impact, rifled launch tubes were used. These tubes were expected to allow both the establishment of projectile flight in the desired orientation by spin stabilization and the removal of a multipiece sabot from the flight path by the spin-generated centrifugal forces. The tubes were nominally 10 ft long with a nominal ID of 0.50 in. The twist rate used was one turn in 20 ft. The rifling consisted of eight equally spaced grooves, 0.008 in. deep by 0.147 in. wide.

2.2 TARGETS AND PROJECTILES

The target material used throughout the test was aluminum 1100-0, having a nominal thickness of 2 in., and was furnished by NASA. The projectile (disk) materials were aluminum, titanium, mild steel, and a commercial tungsten alloy (Kennertium®) and were supplied by ARO, Inc. The ℓ/d ratios varied from 0.1 to 1.1, depending upon the material used. The diameter of all disks launched was 0.2 in. Table I gives the physical properties of the projectile and target materials.

2.3 INSTRUMENTATION

The primary velocity measurements were made with a Beckman & Whitley Model 192 high-speed framing camera. This camera has a maximum framing rate of 1.4×10^6 frames/sec. The 10-in. field of view of the camera includes the target face and allows both impact and pre-impact events to be recorded. The most significant pre-impact data to be recorded were the projectile attitudes. A more complete description of this system is given in Ref. 1. A second method of obtaining velocity made use of two sheets of aluminized plastic film located 50 ft apart. These sheets were perforated by the projectile and were used to start and stop a 10-mc chronograph. Again, this system is described in detail in Ref. 1. A third method of obtaining projectile velocity was by the streak camera system described fully in Ref. 2. A sketch of the system and a description of how it is used at this facility is given in Ref. 1.

Toward the end of the test, a one-station, parallel-ray, refocussed shadowgraph system was installed to provide further verification of projectile attitude. The projectile detector used was of the optical barrier type, employing a collimated light source. The shadowgraph was located at a distance of 45 ft from the muzzle of the launcher. For the same purpose, a flash X-ray system was also sometimes used. This system was situated near the muzzle, in the blast tank.

SECTION III
PROCEDURES

3.1 TEST PROCEDURES

The projectile was seated in a sabot (Fig. 2) and inserted into the breech end of the launch tube. The sabot diameter was approximately 0.005 in. larger than the ID of the barrel, this being the result of previous work which had shown that tight-fitting sabots could be launched with a turn rate very nearly that of the launch tube. Figure 3 illustrates the stabilizing characteristics of the rifled launch tubes. This is a photograph of a yaw card that was penetrated by a 1.0-cal-long, 0.5-in.-diam Lexan® slug. It clearly shows the rifling indentations in the slug. The sabot was counterbored to receive the projectile, and, with a light press fit on the circumference, it was assumed that a portion of the spin stabilization imparted to the sabot by the barrel would be transmitted to the projectile.

Sabot stripping was achieved by the use of the rifled launch tube. Typical separation obtained is shown in Fig. 4, which is a photograph of a lead ring (located at a point 10 ft from the muzzle) that was impacted by the four sabot quarters, showing a total separation of approximately 3.5 in.

The beginning of sabot separation and stabilized flight is shown in Fig. 5. This is a flash radiogram of an aluminum disk ($\ell/d = 0.6$) and sabot being launched at a velocity of 23,500 fps. This radiogram was taken at a point approximately 2.5 ft from the muzzle. More conclusive proof of stabilized flight is shown in Fig. 6. This is a shadowgram of an aluminum disk ($\ell/d = 0.7$) at a velocity of 22,600 fps. This shadowgram was taken at a point 45 ft from the muzzle and 12 ft from the target.

The targets (2-in.-thick 1100-0 aluminum) were mounted at the rear edge of the field of view of the high-speed framing camera and normal to the projectile line of flight. The target specimens were supported so that the rear faces were free of any encumbrances. Throughout the entire test, only those targets impacted by the high ℓ/d tungsten projectiles exhibited a distortion of the rear face. In no case did the rear face distortion exceed 1/8 in.

All testing reported here was at a range tank pressure of from 1 to 2 mm Hg.

3.2 DATA REDUCTION PROCEDURES

The velocity and impact crater data reduction procedures are fully described in Ref. 1. The accuracies, and their derivations, of all velocity measuring systems and the crater measuring system are also given in Ref. 1. In summation, the errors in time and distance allow an absolute velocity determination within one percent error limits with the high-speed framing camera. The velocity measurement variations between the high-speed framing camera and the aluminized film system range from 0 to 3.7 percent, based on previous experience. The streak camera system yields velocity measurements which fall within 0.9 to 4.6 percent of those from the high-speed framing camera; again, this figure is based on previous work.

SECTION IV
RESULTS AND DISCUSSION

Velocity and crater dimensions for tests with all projectile-target combinations are given in Tables II through V. Except where otherwise indicated, the velocity figures which appear in these tables are those which resulted from the use of the high-speed framing camera.

4.1 IMPACT PHENOMENA

The phenomena of hypervelocity impact have been described by Christman and others by a model which breaks down into four stages. They are, from Ref. 3:

1. First (transient): Impact velocity and Hugoniot properties are the only significant parameters in establishing the pressures acting on the projectile and target.
2. Second (steady-state or primary penetration): The densities and compressibilities of the projectile and target, as well as velocity and dimensions of the projectile, enter into evaluation of the intensity and duration of the pressure pulse.
3. Third (cavitation or secondary penetration): This stage is so important in very high-speed impact that neither density nor compressibility appear to be important on the basis of published calculations. This stage continues until the energy behind the shock wave becomes too small to overcome the resistance to deformation of the material.

4. Fourth: This stage is characterized by the reaction of the target material after the stress wave has been attenuated to a level that no longer causes flow or gross plastic deformation of the target material. This stage is not considered in most theoretical approaches.

It has been further stated (Ref. 3) that for projectiles having a length-to-diameter ratio appreciably greater than unity, an extended region of nearly steady-state penetration can be expected (stage two, above). However, for projectiles having length-to-diameter ratios less than unity (disks), the rarefaction wave reflected from the rear projectile surface should reach the projectile-target interface before the steady-state regime can be established. As a result, it is supposed that the steady-state stage is unimportant, and the resulting crater should be shallow and broad instead of hemispherical (Ref. 3).

The results of the series of tests reported here show an apparent disagreement with the analytical work described above and published in Ref. 3. It is obvious from Fig. 7 that the craters resulting from disk impacts are far from being shallow and broad. This plot of P_D/D_c versus ℓ/d shows that for all cases, except for the aluminum of low ℓ/d, the P_D/D_c ratio is greater than hemispherical ($P_D/D_c > 0.5$). Even for the aluminum disks, it is evident that fineness ratio must be reduced to a value substantially below 0.2 if broad, shallow craters are to result.

The approximate duration (t) of the steady-state regime can be estimated from the relationship given for metallic jets, viz (Ref. 4).

$$t = \frac{\ell}{V_p}\left[1 + (\rho_p/\rho_t)^{1/2}\right]$$

Although this relationship does not include all the variables mentioned earlier in describing the steady-state stage, an approximation of the time can be determined with it. Based on the work herein reported, and for projectile lengths of 0.080 in. (ℓ/d of 0.4), the following durations have been computed for impacts with the aluminum targets used in the testing reported here:

Projectile	Second-Stage Duration, μsec
Aluminum 1100-0	6.6
Titanium	8.7
Steel	12.1
Tungsten	19.0

These computations, taken with the conclusion that the second stage of cratering is important (as argued above on the basis of Fig. 7) would

seem to indicate that durations as small as 6 μsec are important in the cratering process. Although these calculated durations may not be significant in themselves, they may show the order of magnitude of time that can be consumed during the steady-state stage of flat disk impact. It is interesting to note here that these calculated steady-state durations are greater than the periods of the impact flash durations generated in the first (transient) stage (Ref. 5).

Figure 8 is a plot of crater volume/projectile energy as a function of projectile ℓ/d for projectile materials of aluminum, titanium, and tungsten; steel has been omitted because of an excessive data scatter. The data for this plot are tabulated in Table VI. Figure 8 shows an increase in cratering effectiveness for aluminum and titanium until at some point (varying with material) it appears to become independent of the projectile ℓ/d. Tungsten exhibits a different behavior, as seen in Fig. 8. Christman et al. (Ref. 5) attribute an increasing trend in cratering effectiveness of higher ℓ/d projectiles to the fact "... that less rod mass is 'used up' in getting through the transient phase of cratering and establishing the primary (steady-state) penetration phase, and also that the contribution of residual cratering (or cavitation phase) at the bottom of the crater becomes less. This would require that both the transient and cavitation phase be less 'efficient' than the primary stage... Therefore, as the ℓ/d becomes greater, the percentage of rod available for cratering in the primary stage would increase and the crater volume would increase."

Actually, this same argument, by substituting "disk" for "rod", seems applicable to the work reported here. This seems to cast doubt on the reasoning applied to rods in Ref. 5. Indeed, data in Fig. 8, interpreted in the light of Ref. 3, imply that in low ℓ/d impacts the primary (steady-state) phase may be important. The fact that the cratering effectiveness for each material appears to become independent of the projectile ℓ/d can be explained again as is done in Ref. 5; i.e., "... the contribution of the transient and cavitation phases to the total volume becomes so small, compared to the primary phase, that any further decrease becomes insignificant." The most significant difference between the data presented here and those in Ref. 5 is that the increase in cratering effectiveness for this work (Fig. 8) occurs up to ℓ/d values of 0.6 (depending on material) and for the work in Ref. 5, up to ℓ/d values of 3.0.

4.2 CRATER SHAPE

Figure 7 is a plot of P_D/D_c versus ℓ/d. This ratio, P_D/D_c, might well be called the "crater shape" parameter. This figure shows that,

for a given velocity and given target and projectile materials, crater shape is a function of the projectile ℓ/d. The craters in this case become deeper and narrower as the ℓ/d increases. This, according to Ref. 5, is compatible with the jet penetration theory. Contrary to published findings for higher fineness ratio projectiles (Ref. 5), the ratio, P_D/D_c, was not, in the work reported here, found to be directly proportional to the projectile ℓ/d. It appears obvious from Fig. 7 that the higher P_D/D_c ratio craters result from the impacts of the higher density projectiles. One can conclude from this that projectile density does play an important role in the determination of the final crater shape. The most notable facet of Fig. 7 is the higher rate of growth of P_D/D_c for tungsten, as compared with the rates for aluminum, titanium, and steel.

4.3 PENETRATION AND VOLUME

The fact that the depth of penetration and the volume of the crater vary significantly with the density of the projectile has been documented in many reports (e.g., Ref. 6). These reports generally discuss the effect in relation to spherical projectiles. These same considerations are borne out for low-fineness-ratio disks in Figs. 9 and 10. Figure 9 is a least-squares plot of P_D as a function of ℓ/d, and it shows an increase in penetration with: (1) an increase in ℓ/d, and (2) an increase in projectile density. Figure 10 is a plot of crater volume as a function of ℓ/d, and again the fact that crater volume varies significantly with projectile density and ℓ/d is shown. The curves for aluminum and titanium have shapes which would be expected, but the curves for steel and tungsten show double-valued dependency of crater volume on projectile ℓ/d.

The effect of projectile shape on penetration is shown in Fig. 11. The data for Fig. 11 are tabulated in Table VII. This is a plot of the ratio P_D/P_S (penetration of disk/penetration of sphere) versus ℓ/d. The P_S values were calculated, for spheres having masses equal to the corresponding disks, using the Charters and Summers' relationship:

$$P_S = 0.5\ (\rho_p/\rho_t)^{1/3} \cdot \left(\frac{\rho_p V_p^2}{2 S_t}\right)^{1/3}$$

where (Ref. 1)

$$\rho_p = \rho_t = 2.73 \text{ gm/cc}$$

$$V_p = 24{,}100 \text{ fps} = 7.35 \text{ km/sec}$$

$$S_t = 0.3425 \text{ gm-km}^2/\text{cc-sec}^2$$

It is shown in Ref. 1 that the above relationship is accurate to the order of ±10 percent. It is obvious from Fig. 11 that within the scope of the present data, the projectile shape is not an important variable in the determination of penetration. Figure 11 suggests that the penetration of a disk will generally be somewhat less than that of a sphere of equal mass for a given set of impact conditions. This is true for aluminum, titanium, steel, and, to some degree, for tungsten. The curves for all materials tested (excluding the higher ℓ/d values for tungsten) fall very nearly equal, which would tend to indicate that the projectile material is not a critical factor in the "penetration efficiency."

4.4 CRATER DIAMETER GROWTH

Figure 12 is a plot of crater diameter as a function of projectile ℓ/d for the various materials under discussion. Within the limitations of these data, the rate of growth of the crater diameter is a linear function of the projectile ℓ/d, at least for aluminum, titanium, and steel. With this parameter, as with most of the parameters discussed, tungsten exhibits behavior similar to that of the other materials until the ℓ/d ratio of 0.3 is exceeded, and then it deviates. This deviation is perhaps more dramatically presented in Fig. 13, which is a photograph of the damage resulting from impacts with tungsten disks. Here are seen craters found at extremes of the double-valued function of Fig. 12. Results seen in Fig. 12, except for the higher ℓ/d values of tungsten, are in general agreement with those of Ref. 5.

SECTION V
CONCLUSIONS

From the work herein reported, several conclusions would seem apparent. They are:

1. If the durations of the second stage of impact computed on the basis of Ref. 4 are approximately correct, the steady-state stage of hypervelocity impact of disks is significant, and durations as small as roughly 6 μsec may be important.
2. Projectile density (as would be expected) plays an important role in determining the final crater shape.
3. In the present results, crater shape (P_D/D_c) is a function of the projectile ℓ/d for tungsten, steel, and titanium, and is greater than hemispherical (0.5) in targets of aluminum when $\ell/d \gtrsim 0.1$. In the case of aluminum disks $P_D/D_c > 0.5$ for $\ell/d \gtrsim 0.5$.

4. Penetration and crater volume vary significantly with projectile density.
5. The penetration of a disk is generally no greater than that of a sphere of equal mass.
6. The projectile material is not a critical factor in the "penetration effectiveness" when $0.3 \lesssim \ell/d \lesssim 0.9$.
7. Crater diameter is a linear function of projectile ℓ/d for projectiles of aluminum, titanium, and mild steel impacting aluminum. This is not the case for tungsten projectiles.

REFERENCES

1. Payne, J. J. "Impacts of Spherical Projectiles of Aluminum, Stainless Steel, Titanium, Magnesium, and Lead into Semi-Infinite Targets of Aluminum and Stainless Steel." AEDC-TR-65-34 (AD456391), February 1965.
2. Bailey, S. O., Clark, A. B. J., Hall, D. A., and Swift, H. F. "Facilities and Instrumentation of the NRL Hypervelocity Laboratory." NRL R 5271, February 18, 1959.
3. Christman, D. R., Gehring, J. W., Maiden, C. J, and Wenzel, A. B. "A Study of the Phenomena of Hypervelocity Impact." GM DRL TR 63-216.
4. Eichelberger, R. J. "Experimental Test of the Theory of Penetration by Metallic Jets." Journal of Applied Physics, Vol. 27, No. 1, January 1956, pp. 63-68.
5. Christman, D. R., Wenzel, A. B., and Gehring, J. W. "Penetration Mechanisms of High-Velocity Rods." Proceedings of the 7th Symposium on Hypervelocity Impact, p. 169.
6. Liles, C. D. and Goodman, E. H. "Particle-Solid Impact Phenomena." AEDC-TDR-62-202 (AD287808), November 1962.

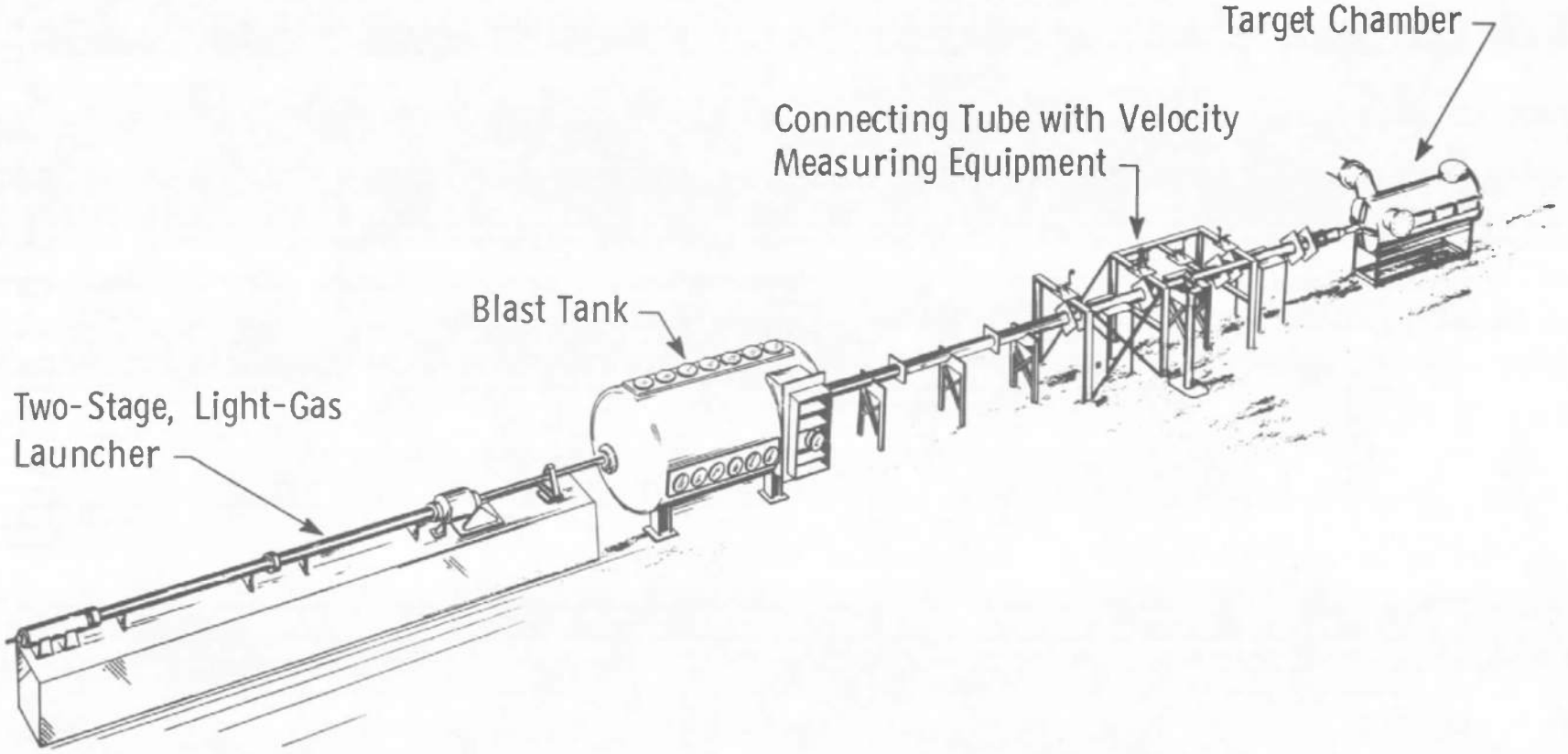

Fig. 1 Armament Test Cell S1

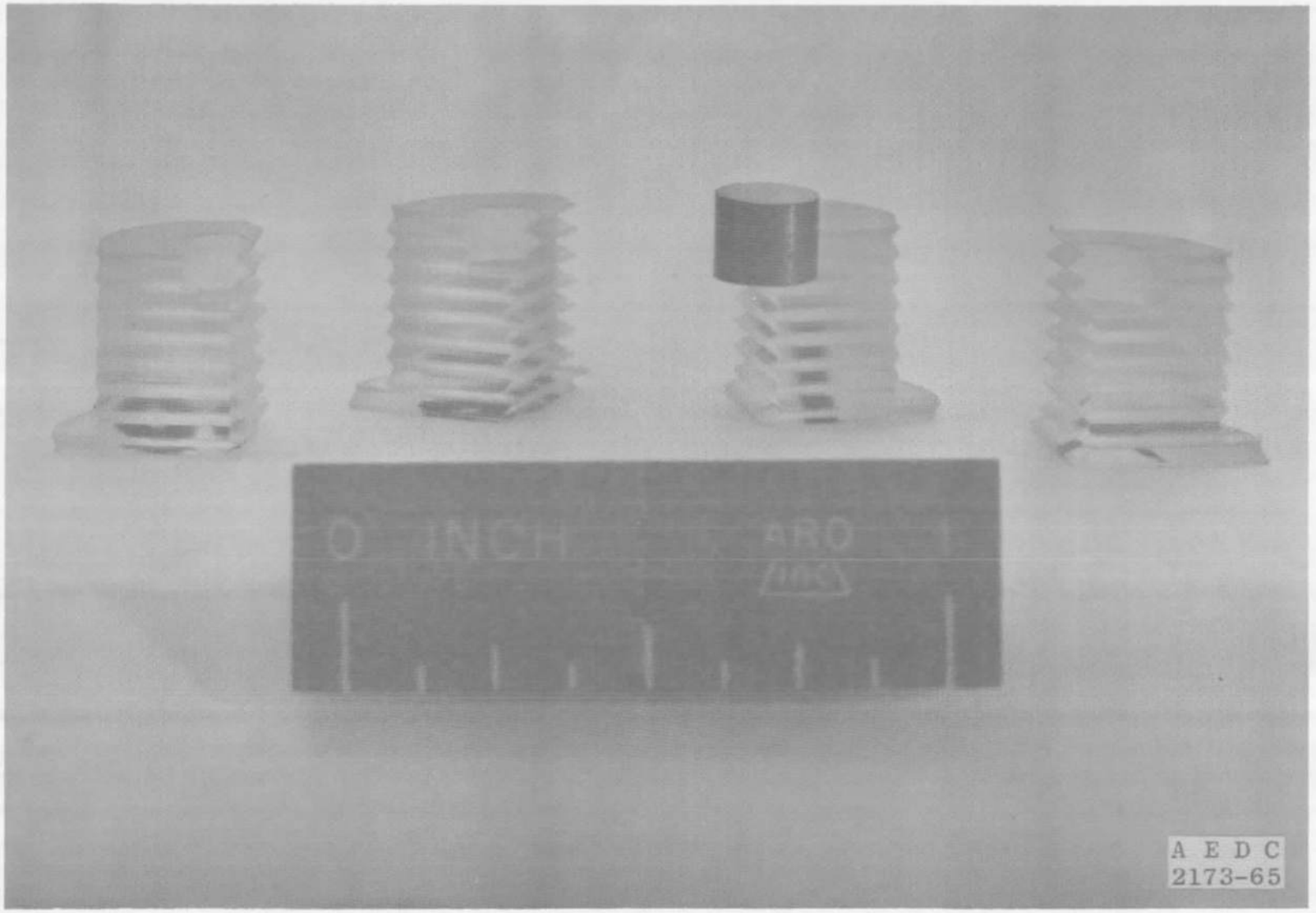

Fig. 2 Projectile and Sabot

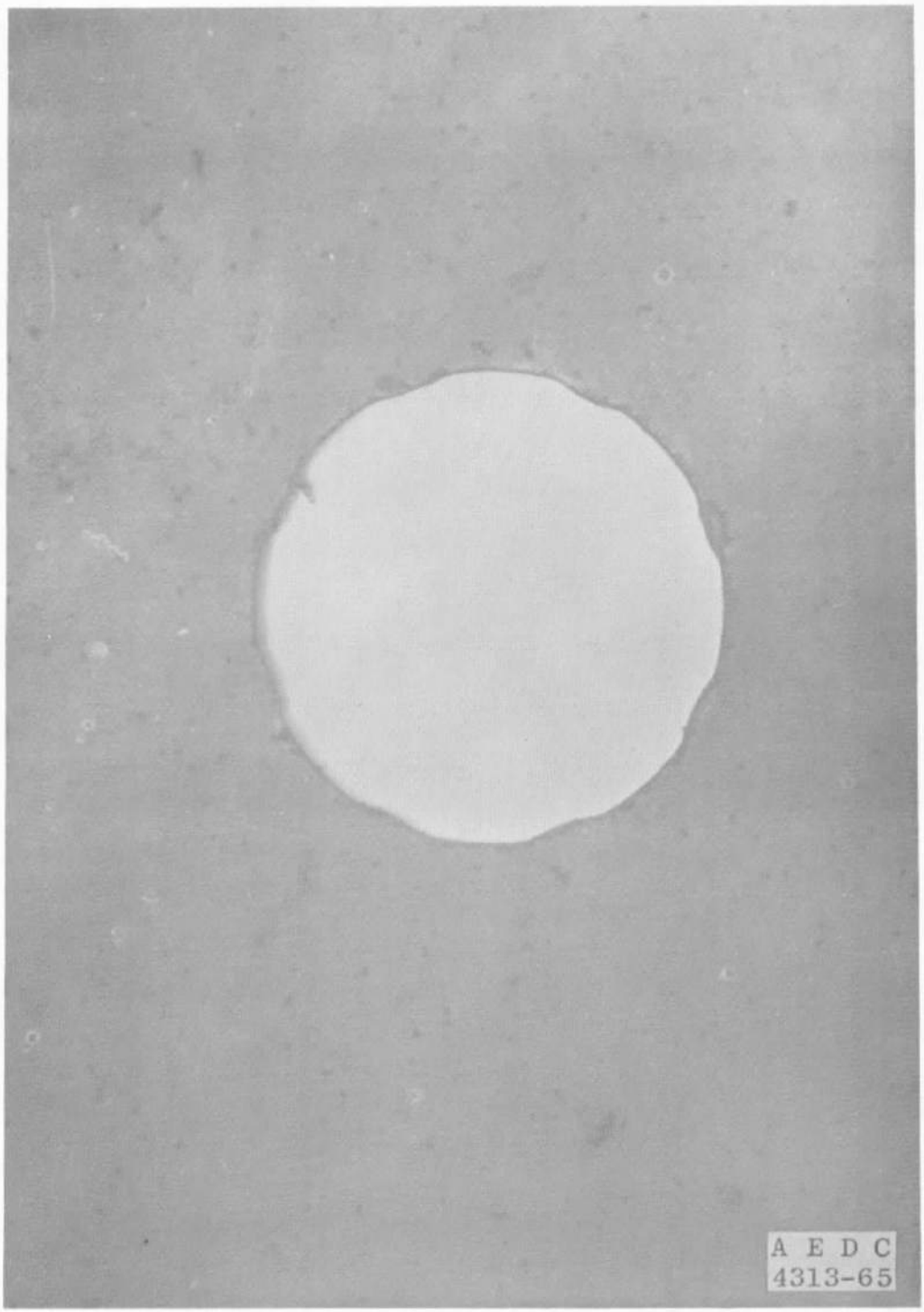

Fig. 3 Yaw Card Shawing Perforation by 1.0-cal-Long, 0.5-in.-Diam Lexan® Slug

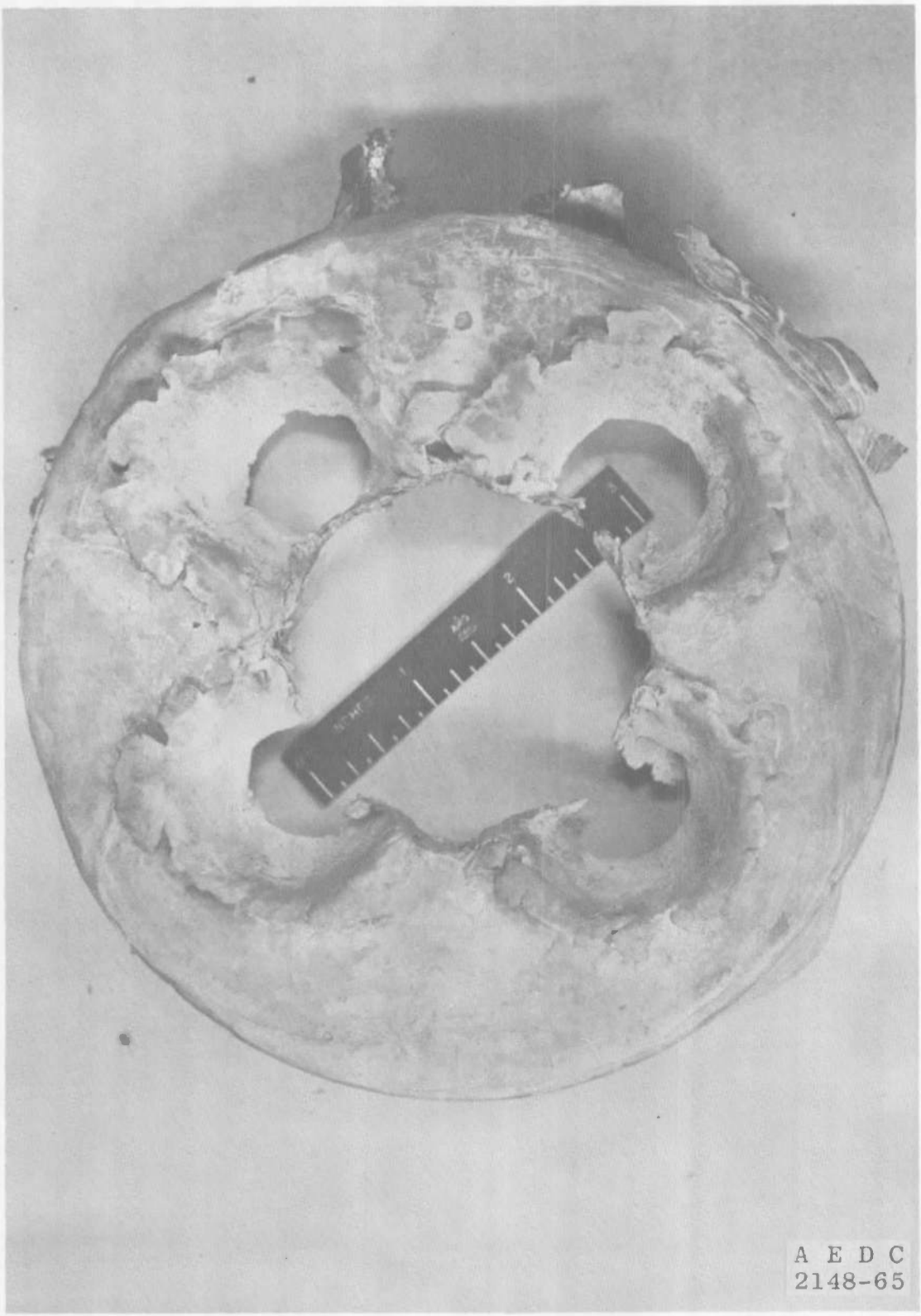

Fig. 4 Lead Ring

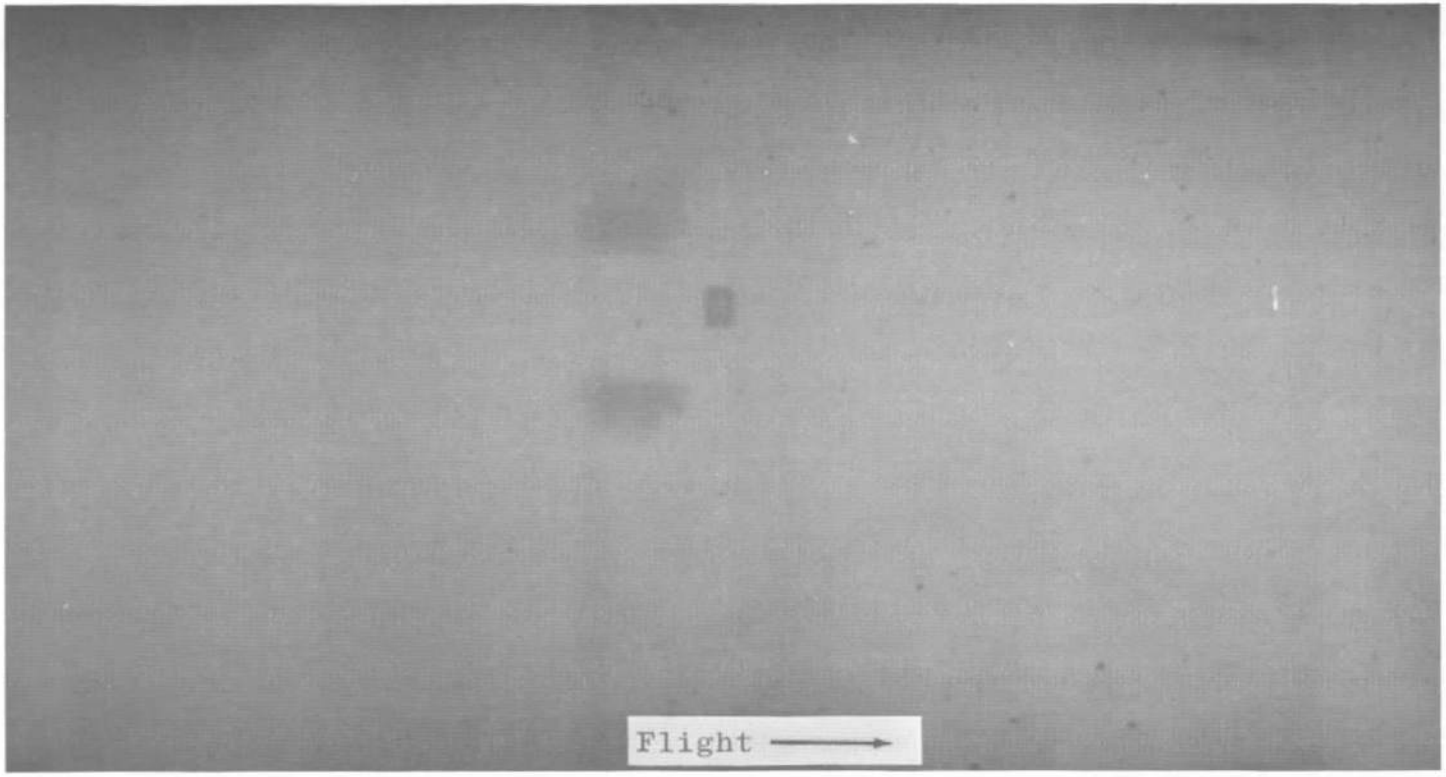

Fig. 5 Flash Radiogram of Projectile and Sabot

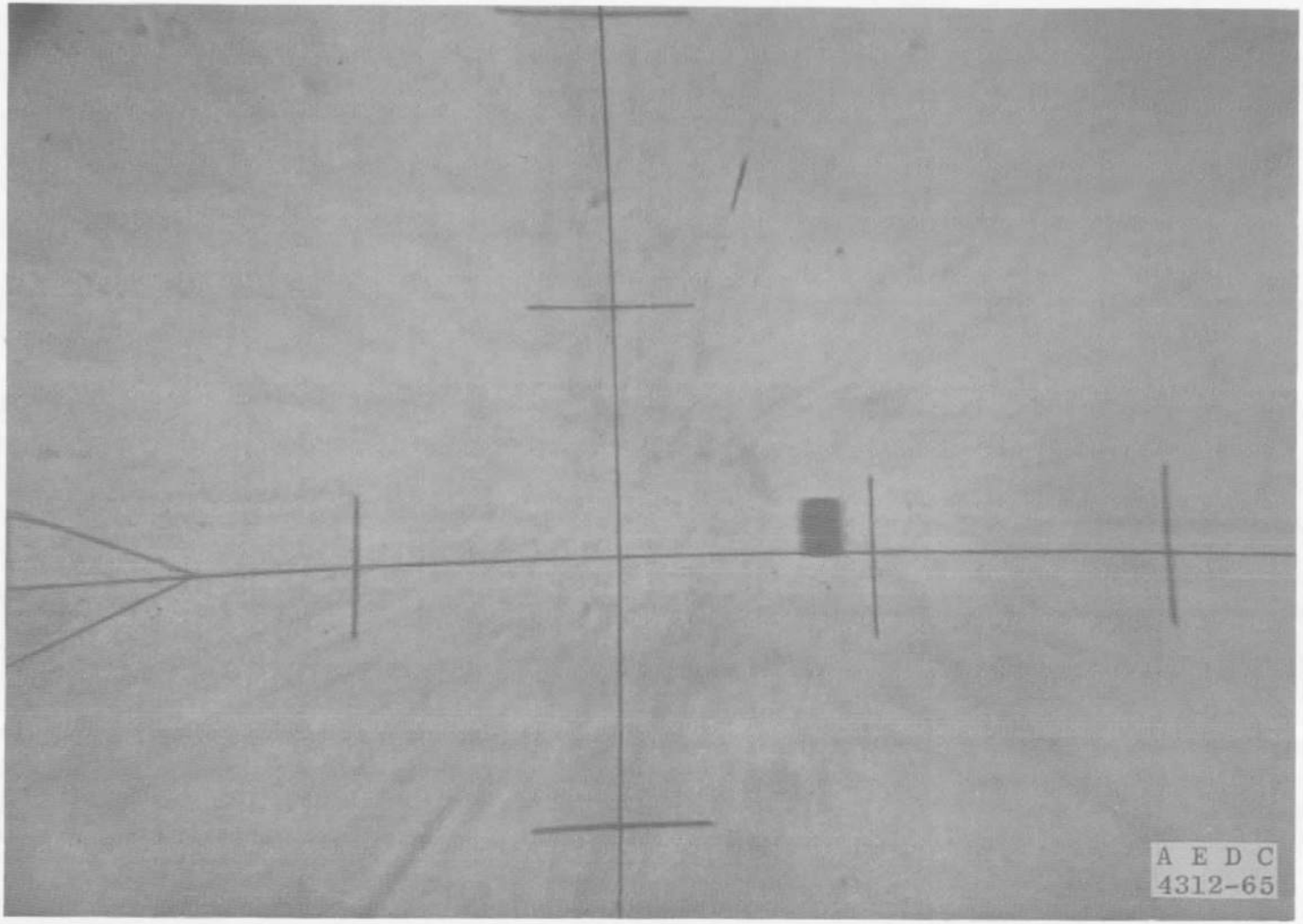

Fig. 6 Shadowgram of a Disk

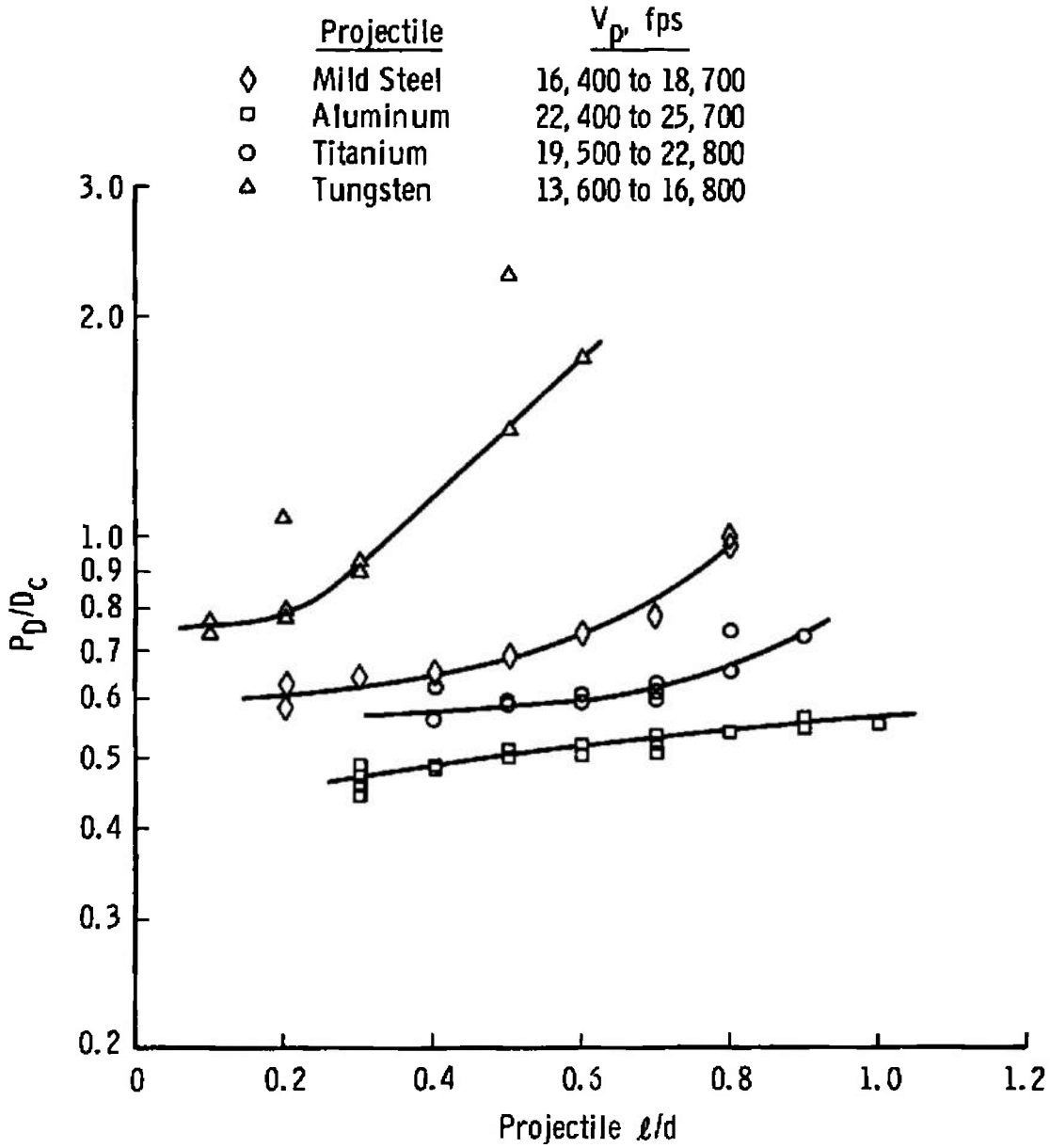

Fig. 7 Crater Shape as a Function of Projectile Fineness Ratio

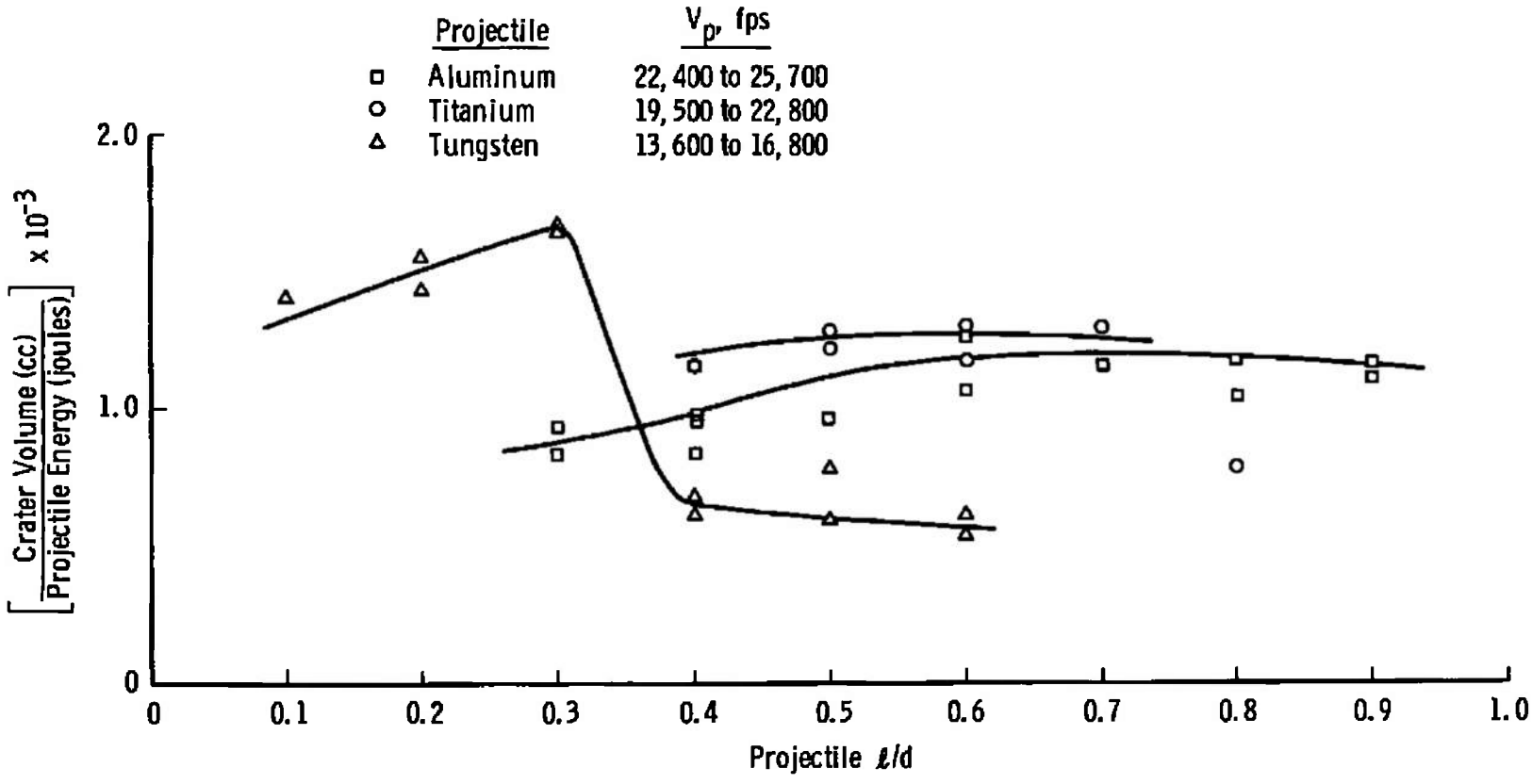

Fig. 8 Cratering Effectiveness as a Function of Projectile Fineness Ratio

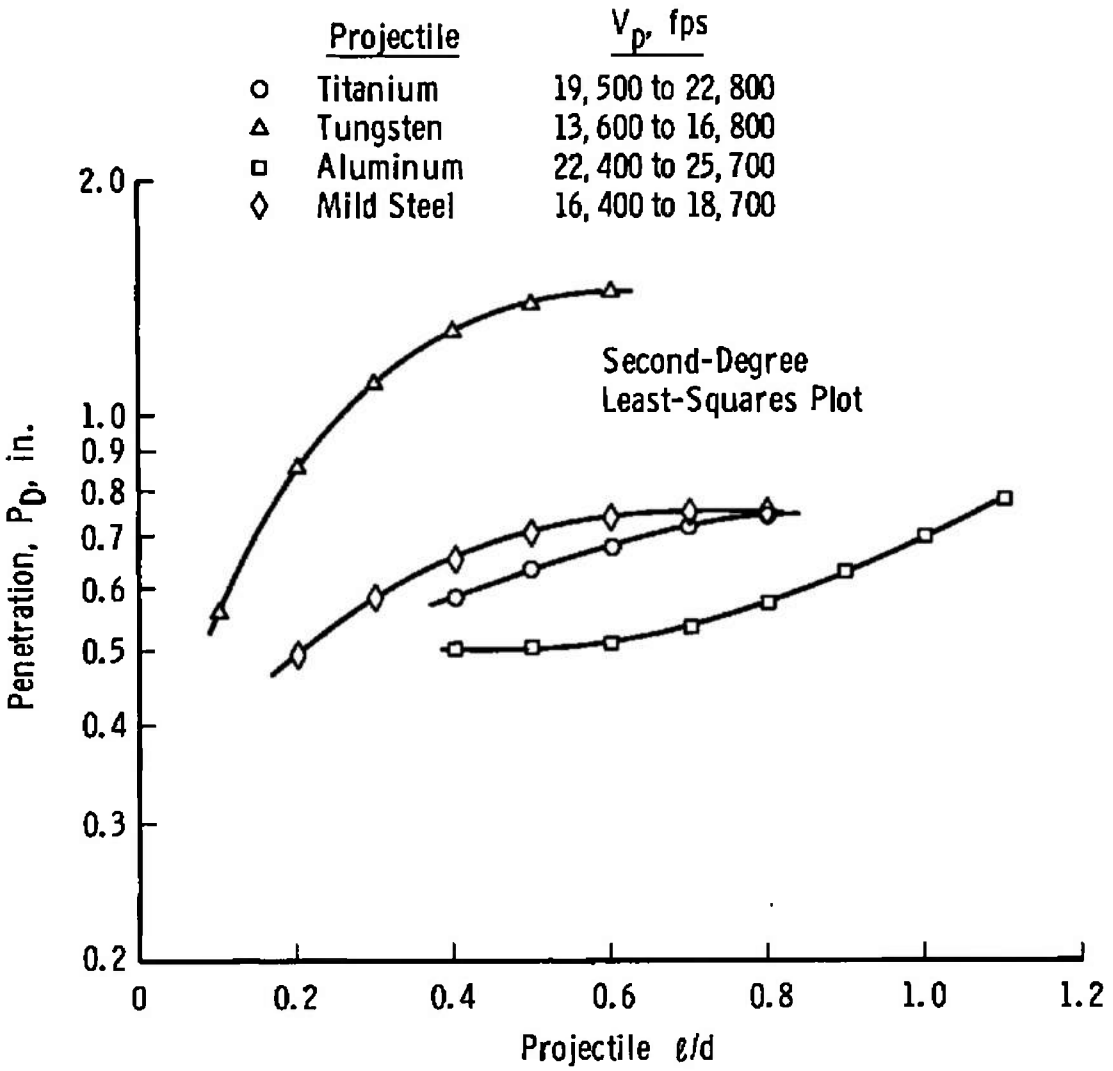

Fig. 9 Penetration as a Function of Projectile Fineness Ratio

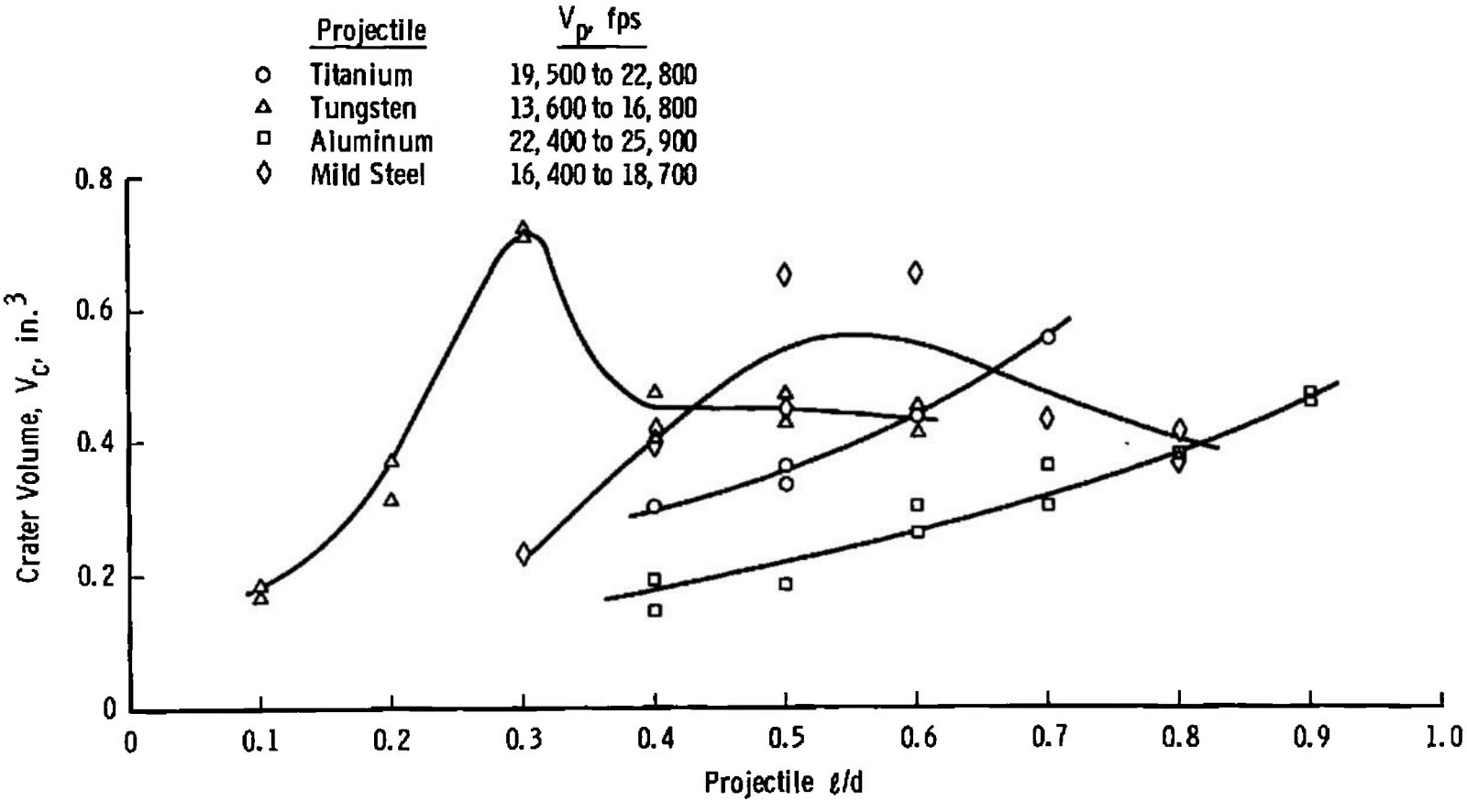

Fig. 10 Crater Volume as a Function of Projectile Fineness Ratio

P_S = Calculated penetration for a sphere of mass equal to the corresponding disk.

P_S Calculated from: $P_S = 0.5\left(\frac{\rho_p}{\rho_t}\right)^{1/3}\left(\frac{\rho_p V_p^2}{2S_t}\right)^{1/3}$

Target Material: Al 1100-0

	Projectile	V_p, fps
□	Aluminum	24, 100
○	Titanium	21, 000
◇	Mild Steel	18, 000
△	Tungsten	15, 000

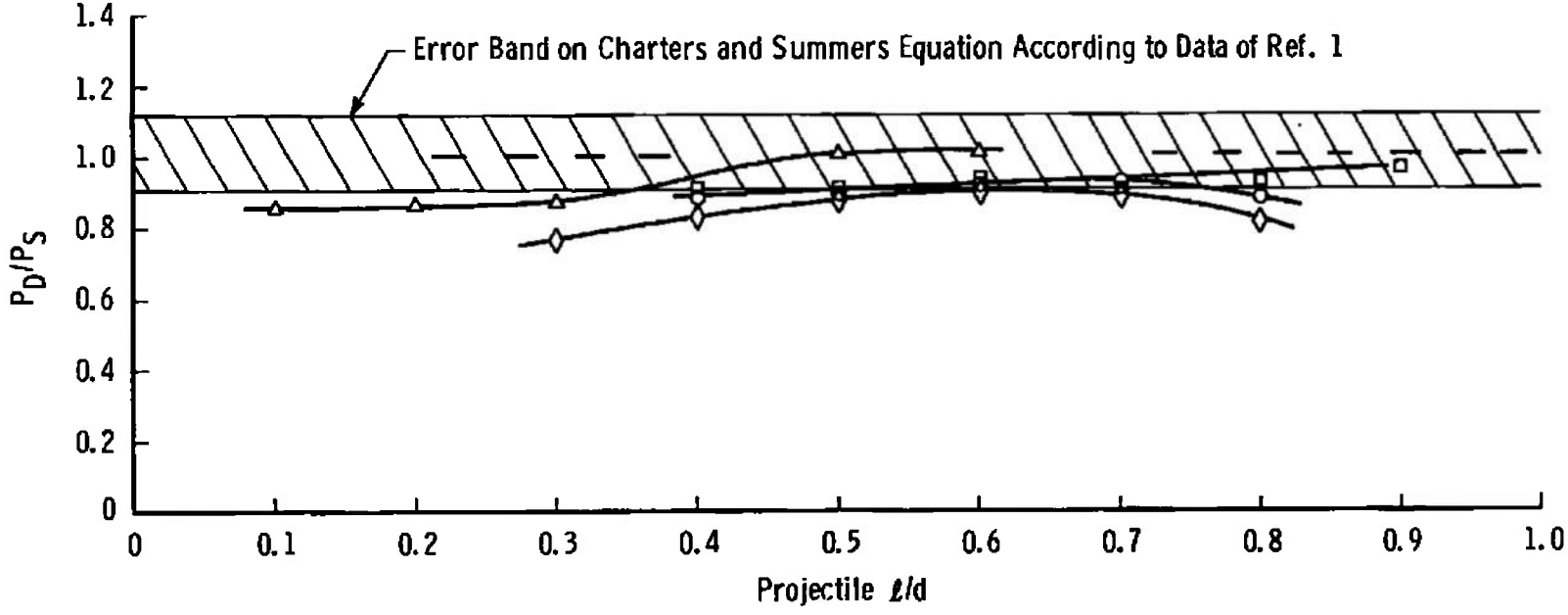

Fig. 11 Normalized Penetration as a Function of Projectile Fineness Ratio

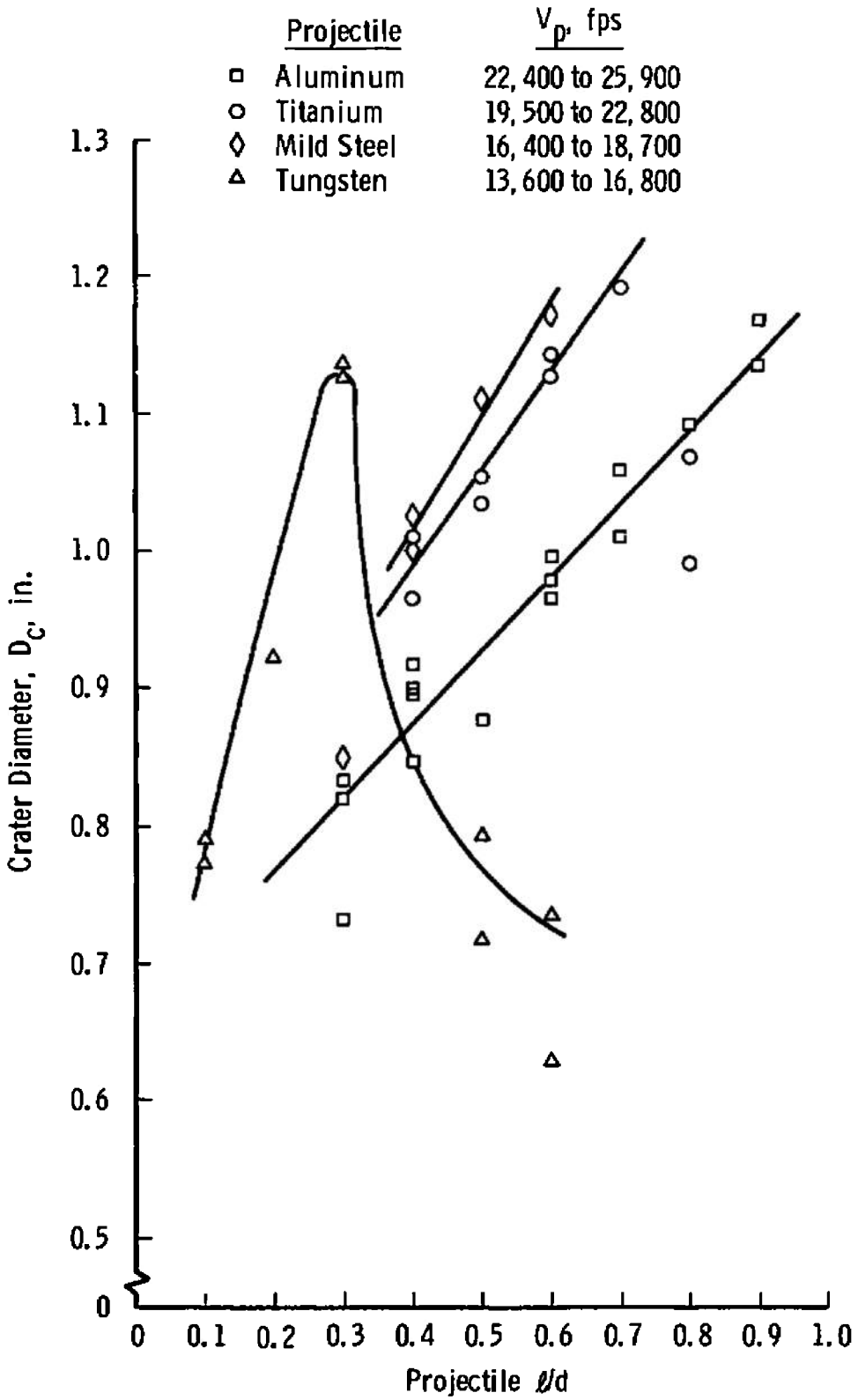

Fig. 12 Crater Diameter as a Function of Projectile Fineness Ratio

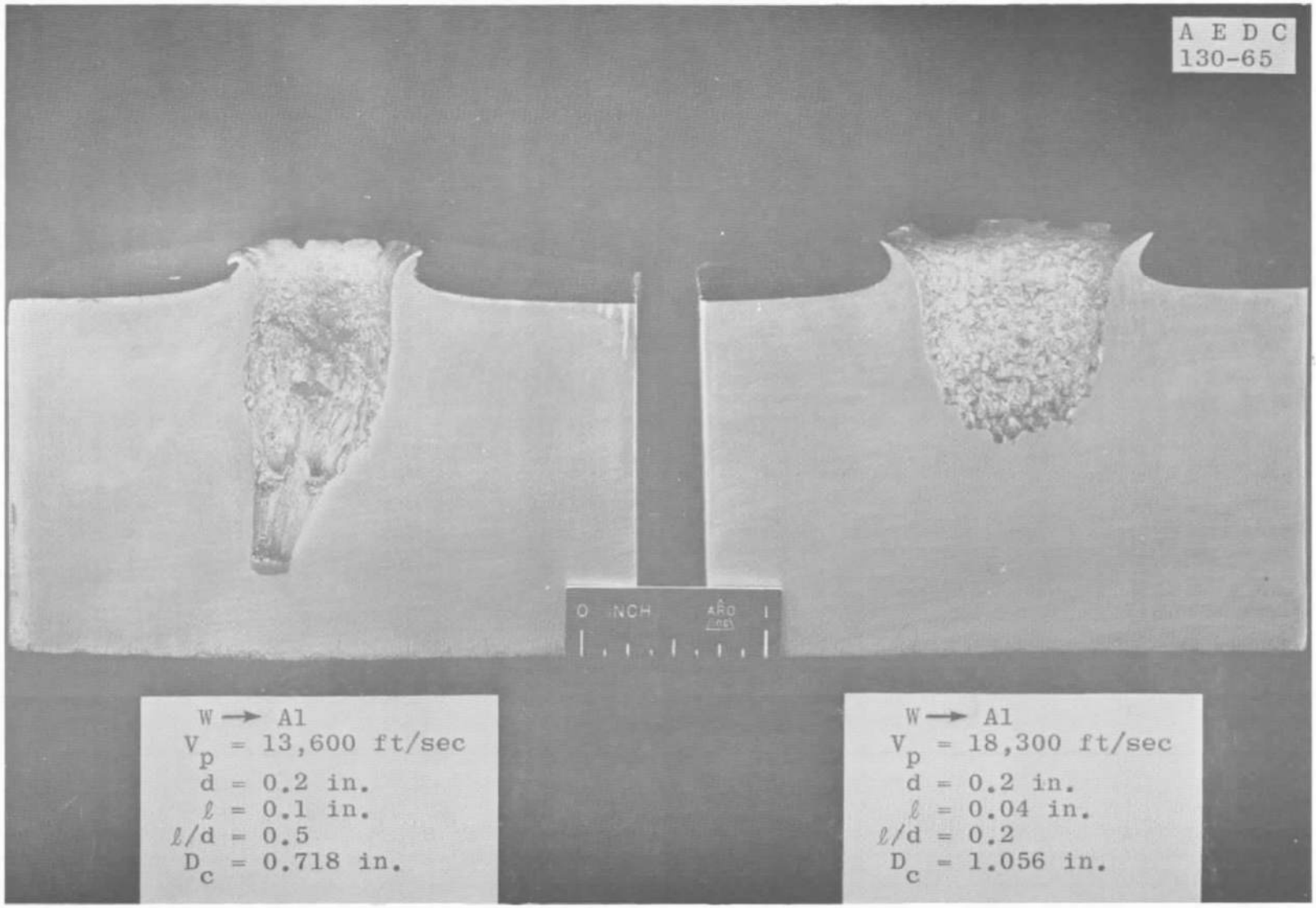

Fig. 13 Sectioned Craters

TABLE I
PHYSICAL PROPERTIES OF PROJECTILE AND TARGET MATERIALS

Material	Rockwell Hardness	Density, gm/cc
Aluminum 1100-0	R_h 42*	2.70*
Titanium	---	4.50*
Mild Steel	---	7.9**
Kennertium (97.6-percent Tungsten)	---	17.9**

*Value measured using standard laboratory techniques

**Manufacturer specifications

TABLE II
VELOCITY AND CRATER DATA FOR 0.2-IN.-DIAM ALUMINUM PROJECTILES

Shot No.	ℓ/d	Velocity, fps	Crater		
			Volume, $in.^3$	Diameter, in.	Depth, in.
168	0.3	16,200	0.0732	0.65	0.316
169	0.3	16,000	0.058	0.629	0.258
172	0.4	13,500	0.061	0.656	0.261
174	0.6	23,200	0.2636	0.9659	0.504
175	0.7	22,200	0.3052	1.0306	0.549
176	0.8	22,700	0.3796	1.093	0.588
177	0.9	23,500	0.4565	1.1367	0.640
191	0.9	24,000	0.4705	1.168	0.636
192	1.0	20,200	0.4351	1.134	0.627
214	0.4	23,200	0.196	0.895	0.492
216	0.5	22,400	0.188	0.878	0.490
217	0.6	23,500	0.304	0.996	0.570
218	0.6	21,300	0.231	0.955	0.484
219	0.7	24,000	0.367	1.101	0.565
227	1.0	17,300	0.328	1.064	0.574
228	1.0	20,900	0.397	1.129	0.625
229	1.1	21,700	0.647	1.185	0.865
255	0.3	20,100	0.1007	0.738	0.345
256	0.4	23,200	0.145	0.846	0.398
257	0.5	20,000	0.151	0.858	0.404
258	1.0	19,400	0.412	1.122	0.618
260	0.6	19,200	0.491	1.166	0.678
263	0.3	18,200	0.080	0.713	0.305
264	0.3	23,400*	0.106	0.732	0.337
267	0.3	25,900	0.143	0.832	0.395
269	0.3	23,900	0.123	0.821	0.369
271	0.4	25,400	0.195	0.918	0.440
272	0.4	24,900	0.186	0.901	0.435
273	0.5	26,000	0.268	1.064	0.533
274	0.5	26,200	0.247	0.999	0.505
275	0.6	25,500	0.246	0.978	0.495
277	0.6	21,900	0.244	0.997	0.494
283	0.7	22,300	0.311	1.032	0.543
284	0.7	22,500	0.303	1.059	0.533

*Aluminized Screen Velocity Measurement

TABLE III
VELOCITY AND CRATER DATA FOR 0.2-IN.-DIAM TITANIUM PROJECTILES

Shot No.	ℓ/d	Velocity, fps	Crater		
			Volume, $in.^3$	Diameter, in.	Depth, in.
184	0.6	23,000	0.5572	1.1851	0.727
185	0.7	18,400	0.4803	1.139	0.709
186	0.8	19,400*	0.4333	1.073	0.713
187	0.9	11,300	0.3009	0.897	0.621
188	1.0	17,100	0.465	1.016	0.743
194	0.8	21,600*	0.412	0.9904	0.739
233	0.4	22,400	0.305	1.010	0.573
234	0.4	22,900	0.302	0.966	0.604
235	0.5	21,800	0.364	1.055	0.624
236	0.5	20,500	0.339	1.034	0.608
237	0.6	21,000	0.453	1.144	0.687
238	0.6	22,300	0.442	1.127	0.670
240	0.7	17,900*	0.554	1.168	0.700
242	0.7	20,600**	0.566	1.192	0.740

*Aluminized Screen Velocity Measurement

**Streak Camera Velocity Measurement

TABLE IV
VELOCITY AND CRATER DATA FOR 0.2-IN.-DIAM MILD STEEL PROJECTILES

Shot No.	ℓ/d	Velocity, fps	Crater		
			Volume, $in.^3$	Diameter, in.	Depth, in.
170	0.2	16,100	0.1318	0.755	0.444
171	0.2	13,800	0.1025	0.685	0.429
195	0.3	21,300	0.3698	1.008	0.654
196	0.4	18,400	0.4156	1.026	0.684
200	0.6	16,300*	0.1928	0.949	0.414
201	0.3	17,300	0.2360	0.8504	0.571
202	0.4	17,300	0.3970	1.004	0.676
203	0.5	17,100	0.4431	1.112	0.764
204	0.6	17,000	0.6518	1.172	0.857
207	0.8	15,900*	0.4290	0.869	0.865
208	0.2	15,200	0.130	0.681	0.472
209	0.5	19,200	0.653	1.206	0.828
210	0.7	19,000*	0.304	0.815	0.641
261	0.7	11,300*	0.362	0.828	0.934

*Aluminized Screen Velocity Measurement

TABLE V
VELOCITY AND CRATER DATA FOR 0.2-IN.-DIAM TUNGSTEN PROJECTILES

Shot No.	ℓ/d	Velocity, fps	Crater		
			Volume, $in.^3$	Diameter, in.	Depth, in.
243	0.1	14,700	0.184	0.772	0.599
245	0.2	18,300	0.522	1.056	0.843
246	0.2	14,900	0.377	0.922	0.850
247	0.3	16,400	0.716	1.129	1.050
248	0.3	16,600	0.7201	1.137	1.032
249	0.4	18,400*	0.472	0.620	1.275
250	0.4	17,300*	0.406	0.635	1.595
251	0.5	16,100*	0.415	0.794	1.10
252	0.5	13,600*	0.476	0.718	1.539
253	0.6	16,700*	0.406	0.631	1.788
254	0.6	15,400*	0.457	0.736	1.294
286	0.1	20,800	0.325	0.9495	0.647
287	0.2	20,100	0.6402	1.108	0.869
290	0.1	15,600	0.168	0.7925	0.599
291	0.2	14,000	0.312	0.9231	0.982
294	0.2	19,100	0.547	1.101	0.879

*Aluminized Screen Velocity Measurement

TABLE VI
ENERGY DATA

Shot No.	Material	ℓ/d	Mass, gm	Velocity, cm/sec x 10^5	Energy, joules	Crater Volume, cc	Crater Volume x 10^{-3} / Projectile Energy
264	Aluminum	0.3	0.0807	7.15	2060	1.74	0.845
269		0.3	0.0834	7.30	2190	2.02	0.925
214		0.4	0.1095	7.10	2760	3.21	1.16
256		0.4	0.1132	7.10	2850	2.38	0.835
271		0.4	0.1090	7.75	3260	3.20	0.982
272		0.4	0.1100	7.60	3180	3.04	0.958
216		0.5	0.1380	6.84	3180	3.08	0.965
174		0.6	0.1601	7.10	4030	4.31	1.070
217		0.6	0.1668	6.86	3920	4.98	1.270
219		0.7	0.1929	7.33	5180	6.0	1.160
284		0.7	0.1935	6.85	4530	4.96	1.050
176		0.8	0.2189	6.93	5250	6.21	1.185
177		0.9	0.2489	7.16	6390	7.48	1.170
191		0.9	0.2501	7.33	6830	7.7	1.125
194	Titanium	0.8	0.3974	6.58*	8813	6.75	0.783
233		0.4	0.1850	6.83	4312	5.00	1.159
234		0.4	0.1850	6.98	4506	4.95	1.098
235		0.5	0.2200	6.64	4857	5.96	1.227
236		0.5	0.2286	6.25	4482	5.55	1.238
237		0.6	0.2747	6.40	5629	7.43	1.319
238		0.6	0.2675	6.80	6182	7.25	1.172
242		0.7	0.3465	6.28	6828	9.29	1.360
243	Tungsten	0.1	0.2128	4.48	2135	3.02	1.414
245		0.2	0.1971	5.58	5972	8.55	1.431
246		0.2	0.3836	4.54	3957	6.18	1.561
247		0.3	0.5595	5.00	6992	11.73	1.677
248		0.3	0.5569	5.06	7127	11.80	1.656
249		0.4	0.7162	5.61*	11,282	7.74	0.687
250		0.4	0.7758	5.27*	10,780	6.65	0.616
251		0.5	0.8360	4.91	11,269	6.80	0.603
252		0.5	1.1184	4.14	9607	7.80	0.811
253		0.6	0.8441	5.09	12,235	6.65	0.543
254		0.6	1.1099	4.70	12,224	7.49	0.612

*Aluminized Screen Velocity Measurement

TABLE VII
EMPIRICAL PENETRATION

Material	ℓ/d	Volume of Disk, cc	Radius of Equivalent Volume Sphere, cm	Diameter of Sphere, in.	Penetration of Sphere, P_S, in.	Penetration of Disk, P_D, in.	P_D/P_S	V_p
Aluminum 1100-0	0.4	0.0369	0.2065	0.1626	0.487	0.438	0.9	24,100
	0.5	0.0503	0.2289	0.180	0.54	0.490	0.908	
	0.6	0.0586	0.2410	0.190	0.57	0.523	0.918	
	0.7	0.0698	0.2571	0.202	0.606	0.549	0.905	
	0.8	0.0803	0.2668	0.210	0.63	0.588	0.932	
	0.9	0.0914	0.2802	0.220	0.66	0.640	0.97	
Titanium	0.3	0.030	0.181	0.1505				21,000
	0.4	0.0411	0.2141	0.1682	0.646	0.573	0.885	
	0.5	0.0498	0.2282	0.18	0.692	0.616	0.890	
	0.6	0.0611	0.243	0.191	0.734	0.676	0.992	
	0.7	0.0772	0.262	0.206	0.79	0.740	0.938	
	0.8	0.0883	0.276	0.218	0.837	0.739	0.882	
	0.9	0.0995	0.288	0.226	0.868			
	1.0	0.1095	0.296	0.232	0.89			
Steel	0.3	0.0292	0.191	0.150	0.743	0.571	0.77	18,000
	0.4	0.0381	0.209	0.165	0.816	0.684	0.836	
	0.5	0.0493	0.228	0.1795	0.889	0.79	0.89	
	0.6	0.0583	0.242	0.191	0.945	0.857	0.907	
	0.7	0.069	0.255	0.202	1.0	0.911	0.911	
	0.8	0.0795	0.268	0.211	1.045	0.824	0.82	
	0.9	0.0896	0.278	0.219	1.085			
Tungsten	0.1	0.0119	0.155	0.0905	0.894	0.599	0.864	15,000
	0.2	0.0214	0.172	0.135	1.045	0.916	0.876	
	0.3	0.0311	0.195	0.1532	1.19	1.04	0.875	
	0.4	0.0433	0.206	0.162	1.25	1.43	1.14	
	0.5	0.0523	0.232	0.184	1.42	1.54	1.08	
	0.6	0.062	0.246	0.1935	1.49	1.54	1.035	

UNCLASSIFIED
Security Classification

DOCUMENT CONTROL DATA - R&D

(Security classification of title, body of abstract and indexing annotation must be entered when the overall report is classified)

1 ORIGINATING ACTIVITY (Corporate author)
Arnold Engineering Development Center
ARO, Inc., Operating Contractor
Arnold AF Station, Tennessee

2a REPORT SECURITY CLASSIFICATION
UNCLASSIFIED

2b GROUP
N/A

3 REPORT TITLE
THE IMPACT OF THIN DISKS INTO SEMI-INFINITE ALUMINUM TARGETS

4 DESCRIPTIVE NOTES (Type of report and inclusive dates)
N/A

5. AUTHOR(S) (Last name, first name, initial)
Payne, J. J., ARO, Inc.

6 REPORT DATE	7a TOTAL NO. OF PAGES	7b. NO. OF REFS
May 1966	37	6

8a CONTRACT OR GRANT NO.	9a. ORIGINATOR'S REPORT NUMBER(S)
AF 40(600)-1200	AEDC-TR-66-35
b. PROJECT NO. 9514	
c System 920E	9b. OTHER REPORT NO(S) (Any other numbers that may be assigned this report)
d	N/A

10 AVAILABILITY/LIMIZATION NOTICES Qualified users may obtain copies of this report from DDC. Release to foreign governments or foreign nationals must have prior approval of NASA.

11. SUPPLEMENTARY NOTES	12. SPONSORING MILITARY ACTIVITY
N/A	National Aeronautics and Space Administration, Marshall Space Flight Center, Huntsville, Alabama

13 ABSTRACT

Hypervelocity impact tests have been performed using aluminum targets and projectiles comprising low-fineness-ratio disks (ℓ/d from 0.1 to 1.0) of 1100-0 aluminum, commerically pure titanium, mild steel, and Kennertium® (97.6 percent tungsten). To ensure the desired projectile attitudes upon impact, rifled launch tubes were used to produce spin stabilization. These tubes allowed the establishment of the desired projectile orientation (their planar surface normal to the flight path) and the removal of a multipieced sabot without a mechanical stripping device. Cratering data for impact velocities from 11,300 to 26,200 fps indicate that the steady-state stage of hypervelocity impact of disks is important and that steady-state duration times of at least 6 μsec are significant. (U)

This document has been approved for pubiic release
its distribution is unlimited. Per AF letter
4 April 1973
signed by W.O. Cole

DD FORM 1 JAN 64 1473

UNCLASSIFIED
Security Classification

14 KEY WORDS	LINK A		LINK B		LINK C	
	ROLE	WT	ROLE	WT	ROLE	WT
impact tests hypersonic projectile crater measurements Disks (1-2) 1. Craters -- Measurements 2. Aluminum targets 3. Craters -- Measurements 4. Impacting						

INSTRUCTIONS

1. ORIGINATING ACTIVITY: Enter the name and address of the contractor, subcontractor, grantee, Department of Defense activity or other organization *(corporate author)* issuing the report.

2a. REPORT SECURITY CLASSIFICATION: Enter the overall security classification of the report. Indicate whether "Restricted Data" is included. Marking is to be in accordance with appropriate security regulations.

2b. GROUP: Automatic downgrading is specified in DoD Directive 5200.10 and Armed Forces Industrial Manual. Enter the group number. Also, when applicable, show that optional markings have been used for Group 3 and Group 4 as authorized.

3. REPORT TITLE: Enter the complete report title in all capital letters. Titles in all cases should be unclassified. If a meaningful title cannot be selected without classification, show title classification in all capitals in parenthesis immediately following the title.

4. DESCRIPTIVE NOTES: If appropriate, enter the type of report, e.g., interim, progress, summary, annual, or final. Give the inclusive dates when a specific reporting period is covered.

5. AUTHOR(S): Enter the name(s) of author(s) as shown on or in the report. Enter last name, first name, middle initial. If military, show rank and branch of service. The name of the principal author is an absolute minimum requirement.

6. REPORT DATE: Enter the date of the report as day, month, year; or month, year. If more than one date appears on the report, use date of publication.

7a. TOTAL NUMBER OF PAGES: The total page count should follow normal pagination procedures, i.e., enter the number of pages containing information.

7b. NUMBER OF REFERENCES: Enter the total number of references cited in the report.

8a. CONTRACT OR GRANT NUMBER: If appropriate, enter the applicable number of the contract or grant under which the report was written.

8b, 8c, & 8d. PROJECT NUMBER: Enter the appropriate military department identification, such as project number, subproject number, system numbers, task number, etc.

9a. ORIGINATOR'S REPORT NUMBER(S): Enter the official report number by which the document will be identified and controlled by the originating activity. This number must be unique to this report.

9b. OTHER REPORT NUMBER(S): If the report has been assigned any other report numbers *(either by the originator or by the sponsor)*, also enter this number(s).

10. AVAILABILITY/LIMITATION NOTICES: Enter any limitations on further dissemination of the report, other than those imposed by security classification, using standard statements such as:

(1) "Qualified requesters may obtain copies of this report from DDC."

(2) "Foreign announcement and dissemination of this report by DDC is not authorized."

(3) "U. S. Government agencies may obtain copies of this report directly from DDC. Other qualified DDC users shall request through _____."

(4) "U. S. military agencies may obtain copies of this report directly from DDC. Other qualified users shall request through _____."

(5) "All distribution of this report is controlled. Qualified DDC users shall request through _____."

If the report has been furnished to the Office of Technical Services, Department of Commerce, for sale to the public, indicate this fact and enter the price, if known.

11. SUPPLEMENTARY NOTES: Use for additional explanatory notes.

12. SPONSORING MILITARY ACTIVITY: Enter the name of the departmental project office or laboratory sponsoring *(paying for)* the research and development. Include address.

13. ABSTRACT: Enter an abstract giving a brief and factual summary of the document indicative of the report, even though it may also appear elsewhere in the body of the technical report. If additional space is required, a continuation sheet shall be attached.

It is highly desirable that the abstract of classified reports be unclassified. Each paragraph of the abstract shall end with an indication of the military security classification of the information in the paragraph, represented as *(TS)*, *(S)*, *(C)*, or *(U)*.

There is no limitation on the length of the abstract. However, the suggested length is from 150 to 225 words.

14. KEY WORDS: Key words are technically meaningful terms or short phrases that characterize a report and may be used as index entries for cataloging the report. Key words must be selected so that no security classification is required. Identifiers, such as equipment model designation, trade name, military project code name, geographic location, may be used as key words but will be followed by an indication of technical context. The assignment of links, rules, and weights is optional.